Research Square

Preprints are preliminary reports that have not undergone peer review.
They should not be considered conclusive, used to inform clinical practice,
or referenced by the media as validated information.

Lymphocyte-specific protein tyrosine kinase contributes to spontaneous regression of liver fibrosis by interacting with suppressor of cytokine signaling1

Hui-zi Zhao
Anhui Medical University
Hong Zhu
Anhui Medical University
Yuan Zhang
Anhui Medical University
Yu-hao Ding
Anhui Medical University
Rui Feng
Anhui Medical University
Jun Li
Anhui Medical University
Cheng Huang
Anhui Medical University
Taotao Ma (mataotao@ahmu.edu.cn)
Anhui Medical University https://orcid.org/0000-0003-2208-2505

Research Article

Keywords: Liver fibrosis, Hepatic stellate cells, Regression. Lymphocyte-specific protein tyrosine kinase, Suppressor of cytokine signaling 1

Posted Date: April 12th, 2022

DOI: https://doi.org/10.21203/rs.3.rs-1420855/v1

License: This work is licensed under a Creative Commons Attribution 4.0 International License.
Read Full License

Abstract

Quiescent hepatic stellate cells (qHSCs), activated to myofibroblasts, produce the fibrous scar is an essential event during liver fibrogenesis. Clinical and experimental fibrosis undergoes a remarkable regression when the underlying etiological agent is removed. Some myofibroblasts revert to an inactive phenotype (iHSCs) during regression of fibrosis. However, the mechanism of HSCs activation and reversal is still obscure. The present study demonstrated the expression of Lymphocyte-specific protein tyrosine kinase (LCK) was increased in fibrotic liver but decreased after spontaneous recovery in vivo and in vitro, and this was correlated with the expression of α-smooth muscle actin (α-SMA) and Type I collagen (COL-1). Further investigation indicated that specific knockdown of LCK by hepatic-adeno-associated virus (AAV9) in C57BL/6 mice ameliorated liver fibrosis. Co-incubation of TGF-β1-induced HSC-T6 with LCK-siRNA inhibited the cell proliferation and activation. Over-expression of LCK hindered MDI-induced HSC-T6 inactivation. Interesting we found LCK interact with suppressor of cytokine signaling 1 (SOCS1) and influenced the expression of p-JAK1 and p-STAT1/3. And LCK has a nagative effect of SOCS1 in liver fibrosis. These data suggest that LCK may play a regulatory role in liver fibrosis by inhibiting SOCS1 and implied LCK as a potential therapeutic target for liver fibrosis treatment.

Introduction

Liver cirrhosis is a major health problem worldwide and short of specific and effective treatments (Ginès et al. 2021). Acting as a precursor to cirrhosis, liver fibrosis (LF) is triggered chronic liver damage produced by hepatitis virus, toxins, drugs, alcohol and so on (Berumen et al. 2021).The hepatic stellate cell (HSC) is a key cell type that contributes to liver fibrosis (Tsuchida et al. 2017).Upon liver insults, HSCs obtain a myofibroblastic phenotype. Myofibroblasts are Type I collagen $(COl1α1)^{+}$ and α-smooth muscle actin $(α\text{-}SMA)^{+}$ cells that produce the extracellular matrix (ECM) in fibrosis. The excessive extracellular matrix disrupts liver cytoarchitecture leading eventually to cirrhosis and liver failure (Tha et al. 2017). One of the most important concepts in clinical and experimental liver fibrosis is reversibility (Calvente et al. 2019; Kisseleva and Brenner 2021; Kisseleva et al. 2012; Krizhanovsky et al. 2008). Promoting activated HSC goes apoptosis or inverts to a quiescent phenotype is a critical step in fibrosis reversion (Bu et al. 2018; You et al. 2021; Yu et al. 2019). However, the mechanism of HSC activation and reversal is still obscure.

Lymphocyte-specific protein tyrosine kinase (LCK) is a member of the Src family of protein tyrosine kinases (Li et al. 2019). A multitude of studies have clarified LCK plays a key role in T-lymphocyte activation and differentiatio (Abraham et al. 1991; Wei et al. 2020). Additional studies have shown that LCK is expressed not only in T cells but also in other cell types (Bommhardt et al. 2019). Talab et al reported that LCK played an important role in mediating B cell receptor signaling in chronic lymphocytic leukemia cells (Talab et al. 2013). Also, Betapudi et al reported LCK regulated endothelial cell survival and angiogenesis (Betapudi et al. 2016).

In this paper, it was revealed LCK was significantly up-regulated in the patient liver tissues. Interestingly, the protein expression of LCK was also increased in liver tissues of CCl_4-treated mice and restored in reversal group, which correlated with the expression of α-SMA and Col1α1. Specific knockdown of LCK by hepatic-adeno-associated virus (AAV9) in C57BL/6 mice ameliorated liver fibrosis *in vivo*. Similarly, knockdown of LCK by siRNA inhibited TGF-β1-induced proliferation of HSC, while overexpression of LCK inhibited activated HSC going to a quiescent type *in vitro*. Furthermore, LCK interact with SOCS1, an important negative regulatory protein in the Janus kinase (JAK)/STAT activator pathway and has a negative feedback function on JAK/STAT1/3 (Liau et al. 2018). LCK influenced the expression of p-JAK1 and p-STAT1/3 has a nagative effect of SOCS1 in liver fibrosis. Thus, this study provided evidence of LCK as a novel antifibrotic therapeutic target during liver fibrosis.

Materials And Methods

Materials and reagents

Antibodies specific for LCK, SOCS1 were purchased from Abcam (Abcam, Cambridge, UK). The antibodies for α-SMA, Col1α1, JAK1, p-JAK1, STAT1, Pp-STAT1, STAT3, p-STAT3 and β-actin were purchased from Bioss Biotechnology (Bioss, Beijing, China). An alanine aminotransferase (ALT) (C009-2-1) assay kit and aspartate aminotransferase (AST) (C010-2-1) assay kits were purchased from Nanjing Jiancheng Bioengineering Institute (Nanjing, China). TGF-β1 was purchased from Peprotech (New Jersey, USA). An Annexin V-FITC Cell cycle analysis kit (BB-4104), and Cell Counting Kit-8 (CCK-8) (BB-4202) were obtained from BestBio (Shanghai, China). Mouse Hyaluronic Acid (HA), laminin (LN) and Type 3 procollagen (PCIII) ELISA kits were obtained from jymbio (Jiyinmei Biotechnology, Wuhan, China).

Mouse models of CCl4-induced liver fibrosis

Male C57BL/6J mice (six- to eight-week-old) were obtained from the Experimental Animal Center of Anhui Medical University. All animal procedures were approved by the Institutional Animal Experimental Ethics Committee. Mice were randomly allocated to each group, food and water were freely available throughout the experiments and maintained in a 12-h light/12-h dark cycle. Liver fibrosis was established by intraperitoneal injection of CCl_4 (0.001 ml/g, CCl_4 dissolved in olive oil at a ratio of 1: 4), biweekly for 4 weeks. Control mice were injected with the same volume of olive oil. The reversal model was kept normal feeding for 6 weeks after CCl_4 stop. Then, serum samples and liver tissues were collected for further analysis.

Adeno-Associated Virus 9 Mouse Model

Luciferase-labelled specific liver tissue location of rAAV9-shLck and vector were designed and obtained from Hanheng (Shanghai, China). All mice were randomly divided into 5 groups (n = 6 per group): vehicle group, CCl_4 group, rAAV9-NC group, rAAV9-NC + CCl_4 group, and rAAV9-shLCK + CCl_4 group. Two weeks later, mouse LF model was established for 4 weeks after rAAV9 administration. Mice exposed to rAAV9 delivery were anaesthetized, effect of rAAV9-shLCK on liver tissue location was confirmed using an IVIS

Lumina III Imaging System (Caliper Life Sciences, USA). Vehicle group mice were administered intraperitoneal injection olive oil biweekly. CCl_4 group was induced by CCl_4 intraperitoneal injections (0.001ml/g) biweekly. rAAV9-NC group mice were injected with an empty rAAV9 vector by tail vein injections and intraperitoneal injection olive oil. rAAV9-shLCK group mice were injected with an rAAV9-shLCK vector by tail vein injections and intraperitoneal injection olive oil. AAV9-NC + CCl_4 group mice were injected with an empty rAAV9 vector by tail vein injections and CCl_4 intraperitoneal injections (0.001ml/g) biweekly. rAAV9-shLCK + CCl_4 group mice were injected with an rAAV9-shLCK vector by tail vein injections and CCl_4 intraperitoneal injections (0.001ml/g) biweekly. Then, collected serum samples and liver tissues which were paraformaldehyde-fixed and paraffin-embedded.

Cell culture and cell treatment with TGF-β1

HSC-T6 cells, the rat HSCs, were obtained from Procell Life Science & Technology (Wuhan, China). HSC-T6 cells were cultured in Dulbecco's modified Eagle's medium (DMEM, HyClone, USA), supplemented with 10% fetal bovine serum (FBS, Every Green, China) and incubated at 37°C with 5% CO_2. HSC-T6 cells were induced by 10 ng/ml TGF-β1 for 48 h.

MDI treatment

In vitro activation of HSC-T6 was achieved by co-culturing HSC-T6 cells with TGF-β1 (10 ng/ml) for 24 h. After that, they were treated with the adipogenic differentiation mixture (MDI, 0.5 mM isobutylmethylxanthine (Sigma-Aldrich, St. Louis, MO, USA), 1 μM dexamethasone (Sigma-Aldrich, St. Louis, MO, USA), and 1 μM insulin (Sigma-Aldrich, St. Louis, MO, USA)) and incubated for 48 h.

Histopathology and immunohistochemistry staining

Paraformaldehyde-fixed, paraffin-embedded liver tissues were sectioned (5 μm) for H&E and Masson and immunohistochemical (IHC) staining for α-SMA and Col1α1. Slides were scanned by an automatic digital slide scanner (Pannoramic MIDI, 3DHISTECH, Hungary) and analysed by the CaseViewer software. The positive staining areas were measured by Ipwin32 software.

Immunofluorescence staining

To discover LCK and SOCS1 location in liver tissues, frozen liver tissues of mice were blocked with 10% BSA at 37°C for 30 min to avoid nonspecific staining. Then, the sections were incubated with mixture of rabbit polyclonal primary antibodies for LCK (1:100) or SOCS1(1:100) and mouse polyclonal primary antibodies for α-SMA (1:400) at 4°C overnight. Sections were then incubated with a secondary conjugated antibody (1:100) in the dark at room temperature for 1 h. The nuclear staining was achieved by dropping DAPI for 5min. The stained sections were examined by inversion fluorescence microscopy until tissue section were dry.

To further discover the expression of LCK in non-treated HSCs, TGF-β1-treated HSCs, MDI-treated HSCs in vitro, we performed cell immunofluorescence mono-staining. Three cells groups were washed, fixed, permeabilized and blocked with 5% bovine serum albumin (BSA). The cells were incubated with a rabbit monoclonal primary antibody for LCK (1:100) at 4°C overnight. The second day, anti-rabbit FITC conjugated secondary antibodies was used to conjugate antigen combined LCK for 1h at room temperature. The cells were counterstained with DAPI and visualized using fluorescence microscopy. Cell nucleus was shown as blue fluorescence and LCK was green fluorescence.

CCK-8 analysis

HSC-T6 cells were seeded into 96-well plates, and the edge wells were filled with PBS. Cells were treated with 10ng/ml TGF-β1 or MDI after transfection with siRNA and pEX-2-LCK. After 24h or 48h,10 μl CCK-8 (Shanghai, China) was added to each well for 4 h. The value of absorbance (A) was examined at a wavelength of 450 nm. The cell viability was calculated according to the formula.

Western blotting

Mice liver tissues (30 or 50 mg) and HSC-T6 cells were lysed with RIPA lysis buffer (Beyotime, China). The protein concentration was determined by using a BCA protein assay kit (Beyotime, Jiangsu, China), according to the instruction manual. Proteins were separated by sodium dodecyl sulfate-polyacrylamide gel electrophoresis (SDS-PAGE) and transferred onto polyvinylidene fluoride (PVDF) membranes (Millipore Corp, Billerica, MA, USA). The PVDF membranes were blocked in 5% skim milk for 1.5 h at room temperature and then, washed three times in TBST. The PVDF membranes were incubated at 4°C overnight with specific primary antibodies which were diluted in Dilution Buffer (Beyotime, China). Rabbit polyclonal anti-Col1α1, α-SMA, JAK1, p-JAK1, STAT1, p-STAT1, STAT3, p-STAT3 and β-actin were diluted at 1:1000, rabbit polyclonal anti-LCK and SOCS1 (Abcam, USA) were diluted at 1:500, followed by incubation with secondary antibodies (1:10000, ZSGB-Bio, China) for 1 hour at room temperature. At last, the protein bands were detected by ECL-chemiluminescent kit (ECL-plus, Thermo Scientific).

Small RNA interference (siRNA) analysis

Small interfering RNA (siRNA) oligonucleotides against the LCK gene or scrambled sequences were designed and synthesized by Hanheng (Shanghai, China). The siRNA sequences were as follows: LCK-siRNA (sense, 5′-GCAUCAAGUUGAA CGUCAATT-3′ and antisense, 5′-UUGACGUUCAACUUGAUGCTT-3′); Scrambled- siRNA (sense, 5′-UUCUCC GAACGUGUCACGUTT-3′ and antisense, 5′-ACGUGA CACGUUCGGAGAATT-3′). HSC-T6 cells were transfected

with 1000 ng/ml LCK-siRNA or scrambled-siRNA and mixed with Lipo2000 transfection

reagent (Invitrogen, USA) according to the manufacturer's instructions. After 6 h, Opti-MEM was replaced by DMEM (10% FBS), and cells were activated by 10 ng/ml TGF-β1. The silencing efficiency was tested by RT-qPCR and Western blot.

Transfection with LCK plasmid

HSC-T6 cells were seeded in 6-well plates and cultured in DMEM (10% FBS). After adhering to the well, the medium was replaced with Opti-MEM (Gbico, USA) and cells were transfected with 1000ng/mL pEX-2-Control and pEX-2-LCK overexpression plasmid mixed with Lipo2000 transfection reagent (Invitrogen, USA) according to the manufacturer's instruction. After 6h, the Opti-MEM was changed to DMEM (10% FBS) contained 10ng/ml TGF-β1. After 24h, use MDI incubated for 48h.

Flow cytometry analysis

Cell cycle analysis kit (Beyotime) was used for cell cycle analysis. In simple terms, HSC-T6 cells were trypsinized, washed with cold PBS, and then, fixed in cold ethanol (75%, 3 mL) at 4°C overnight. Next, the cells were washed twice, treated with a 0.5 ml mixture (RNase and PI), and incubated for 30 min at 37°C in a dark place. A flow cytometer (Beckman, USA) was used to detect the cell cycle, and data were analyzed using FlowJo software (TreeStar, USA).

Co -Immunoprecipitation assay (Co -IP assay)

Co-IP has been successfully used to study the interaction of proteins. Co-IP contains of several steps, including preparation of protein extract, coupling a specific antibody to beads, purification of specific protein complexes. Purified protein compound can then be identified by western blot.

Statistical analysis

Data were represented as Mean ± SD. Statistical analyses were performed using a two-tailed unpaired t test or one-way ANOVA followed by the Newman–Keuls post hoc test (Prism 5 software, USA), p value < 0.05 was considered statistically significant.

Results

LCK promotes CCl_4-induced liver fibrosis

To assess the role of LCK in liver disease, we first analyzed two independent microarray datasets from Oncomine database (Mas et al. 2009; Wurmbach et al. 2007).It was revealed that LCK was significantly upregulated in the liver cirrhosis tissues (Table 1). The median rank of LCK in up-regulated genes of liver cirrhosis was 235 based on a meta-analysis across the two datasets, including 2 analyses using the Oncomine algorithms (Fig. 1a).

Table 1
Detailed information about the 2 public expression datasets of Oncomine database about LCK in liver cirrhosis

TLR	sample size	Type	Fold change	P-value	t-test	References
LCK	Cirrhosis (13)	Cirrhosis vs. Normal	4.485	1.73E-06	6.789	
	Normal (10)					(Mas et al. 2009)
	Cirrhosis (58)	cirrhosis vs. Normal	2.105	1.02E-15	11.09	
	Normal (19)					(Wurmbach et al. 2007)

To examine the functional importance of LCK in liver fibrosis, specific knockdown of LCK by hepatic-adeno-associated virus (rAAV9) in C57BL/6 mice was used (Yang et al. 2018). It was found that fluorescence-labelled rAAV9–LCK was localized in liver (Fig. 1b). ALT and AST, two serum markers of hepatocyte death and liver injury, were obviously down-regulated in rAAV9–LCK-treated liver fibrosis mice (Fig. 1c, d). H&E staining showed the livers from rAAV9–LCK-treated liver fibrosis mice exhibited weakened steatosis and necrosis compared to CCl_4-treated mice (Fig. 1e). Moreover, the serum HA, LN and PCIII levels were obviously down-regulated in rAAV9–LCK-treated liver fibrosis mice (Fig. 1f-h). Consistently, deposition of collagen was decreased in rAAV9-LCK treated liver fibrosis mice examined by masson staining and IHC assay analysis (Fig. 1i, j). These results indicated that knockdown LCK had a protective effect on CCl_4-induced liver fibrosis.

Regression of liver fibrosis is accompanied by loss of LCK in vivo and in vitro

Next, we examined the role of LCK as a potential mediator of spontaneous regression model of liver fibrosis. First, the mice were subcutaneous injection for 4 weeks with CCl_4 to induce liver fibrosis model. After 4 weeks, stop providing CCl_4 to establish the spontaneous regression model of liver fibrosis for another 6 weeks (Fig. 2a). Serum ALT and AST were obviously downregulated in spontaneous regression model of liver fibrosis (Fig. 2b, c). H&E staining showed the livers from spontaneous regression model of liver fibrosis exhibited weakened steatosis and necrosis (Fig. 2d). Moreover, the serum HA, LN and PCIII levels were obviously down-regulated in spontaneous regression model of liver fibrosis (Fig. 2e-g). Consistently, deposition of collagen was decreased in spontaneous regression model of liver fibrosis examined by masson staining and IHC assay analysis (Fig. 2h-j). Interestingly, the protein expression of LCK was up-regulated in liver tissues of CCl_4-treated mice and restored in reversal group, which was in accord with the expression of Col1α1 (Fig. 2k).

The activation of quiescent hepatic stellate cells (qHSC) into myofibroblast-like cells (activated HSC, aHSC) is a pivotal step for the progression of hepatic fibrosis. One of the most important characteristics of the recovery of liver fibrosis is the reversal of aHSC to inactive phenotype (iHSC). Myofibroblast marker

α-SMA was up-regulated in liver tissues of CCl_4-treated mice and restored in reversal group, which were examined by IHC assay and western blot (Fig. 3a, b). Furthermore, we assessed the colocalization of LCK with α-SMA by immunofluorescence staining, finding that LCK was colocalized with α-SMA in HSC (Fig. 3c).

To confirm the expression of LCK in aHSC and iHSC, HSC-T6 cells were treated with TGF-β1 in advance, and 24 hours later, the cells were treated with MDI for another 48 hours (Fig. 4a). The protein levels of Col1α1 and α-SMA were up-regulated in TGF-β1-treated group, but down-regulated in MDI-treated group (Fig. 4b). Interestingly, western blot analyses demonstrated that the protein level of LCK was in accord with α-SMA and Col1α1 (Fig. 4c). Similar result was found in immunofluorescence staining (Fig. 4d).

These results indicated that spontaneous regression of liver fibrosis accompanied by loss of LCK.

Knockdown of LCK inhibited the proliferation of HSC

To evaluate the role of LCK as a potential mediator of liver fibrosis, we treated the TGF-β1-induced HSC-T6 cells with siRNA-based knockdown of LCK for 24 hours (Fig. 5a) and confirmed by western blot (Fig. 5b). Knockdown of LCK had significantly inhibited cell viability by CCK-8 analysis (Fig. 5c). Similarly, western blot analysis showed that siRNA-LCK treatment significantly decreased the protein levels of α-SMA, Col1α1 (Fig. 5d). Furthermore, wound healing assays indicated that siRNA-LCK showed slower rates of wound healing (Fig. 5e). Additionally, cell cycle analysis showed that treatment with siRNA-LCK resulted in an increased percentage of activated HSC-T6 cells in the G0/G1 phase and decreased the population of cells in the G2 phase (Fig. 5f). Similarly, the expression of α-SMA was significantly down-regulated in rAAV9–LCK-treated liver fibrosis mice by IHC assay analysis (Fig. 5g). Hence, knockdown of LCK may inhibit the activation and proliferation of HSC.

Overexpression of LCK inhibited activated HSC going to inactivated phenotype

Next, we treated the TGF-β1-induced HSC-T6 cells for 24 hours, then with MDI and pEX-2-LCK for 48 hours (Fig. 6a) and confirmed by western blot (Fig. 6b). Overexpression of LCK with addition of MDI significantly promoted cell viability compared to a control plasmid by CCK-8 analysis (Fig. 6c). Similarly, western blot analysis showed that overexpression of LCK with addition of MDI significantly increased the protein levels of α-SMA, Col1α1 compared to a control plasmid (Fig. 6d). Furthermore, wound healing assays indicated that overexpression of LCK with addition of MDI showed faster rates of wound healing compared to a control plasmid (Fig. 6e). Additionally, cell cycle analysis showed that overexpression of LCK with addition of MDI decreased percentage of activated HSC-T6 cells in the G0/G1 phase and increased the population of cells in the G2 phase in comparison to a control plasmid (Fig. 6f). Hence, overexpression of LCK with addition of MDI obstructed the regression of activated HSC.

LCK interacted with SOCS1

Venkitachalam et al reported LCK-induced cellular transformation could be suppressed by SOCS1, and SOCS1 has the high affinity in binding to the oncogenic LCK kinase(Venkitachalam et al. 2011). According to the result from co-immunoprecipitation (Co-IP), it was found that LCK protein interacted with SOCS1 (Fig. 7a). Western blot analysis showed that higher levels of phosphorylated JAK-1 and STAT 1/3 in CCl_4 group, yet they were decreased in the rAAV9–LCK-treated liver fibrosis mice (Fig. 7b). Similar observations were found for the vitro model. The expression levels of p-JAK1 and p-STAT1/3 were markedly decreased by siRNA-LCK treatment compared to TGF-β1-induced HSC-T6 cells (Fig. 7c). Furthermore, the expression levels of p-JAK1 and p-STAT1/3 were markly increased by pEX-2-LCK treatment compared to MDI treated group (Fig. 7d).

Interestingly, localization studies demonstrated that the expression level of SOCS1 was down-regulated with the treatment of CCl_4, while a more pronounced increase was observed in spontaneous regression (Fig. 8a). Consistent with in vivo studies, in vitro data were also confirmed in HSC-T6 that SOCS1 level was down-regulated in TGF-β1-treated group and restored in MDI-treated group (Fig. 8b). Additionally, knockdown LCK promoted SOCS1 expression while overexpression of LCK decreased the expression of SOCS1 (Fig. 9a, b). The results were opposite of p-JAK1 and p-STAT1/3. Consistently, double immunofluorescence staining showed that the expression of SOCS1 was significantly up-regulated in rAAV9–LCK-treated liver fibrosis mice (Fig. 9c). The data above indicated that LCK may contribute to aggravate liver fibrosis by suppressing SOCS1 signal pathway.

Discussion

In hepatotoxic-induced liver fibrosis (such as CCl_4), quiescent hepatic stellate cells (α-SMA$^-$Col$^-$qHSC) undergo activation to become the major source of myofibroblasts (α-SMA$^+$Col$^+$aHSC). Myofibroblasts rapidly emerge in fibrotic liver to produce the fibrous scar (Bu et al. 2021).Clinical and experimental hepatic fibrosis regresses dramatically with removal of the underlying etiological agent(Li et al. 2016; Liu et al. 2016).Accumulating evidence indicates that senescence and apoptosis of activated HSC (aHSC) plays a significant role in resolution (Wang et al. 2020).Kisseleva and colleague demonstrated that some aHSC lost expression of fibrogenic genes and persisted in the liver in an inactivated phenotype (iHSC), suggesting that inactivation of aHSC/myofibroblasts is a common feature of regression of liver fibrosis. Therefore, it will be of great significance for the recovery of liver fibrosis to identify the underlying mechanism (Kisseleva et al. 2011).However, we are still at the beginning understanding of the mechanisms of HSC activation and reversal because of its complexity.

LCK, a 56 kD protein tyrosine kinase in the Src family (Yamaguchi and W.A. 1996)., is an important reproduction related gene (Zepecki et al. 2018). LCK has long been recognized to be potent oncoproteins and its activation is often associated with cell activation, growth, proliferation and transformation(Li et al. 2019) (Shi et al. 2006).Liu et al reported LCK inhibitor attenuated atherosclerosis in ApoE$^{(-/-)}$ mice and reverse cholesterol transport(Liu et al. 2020).The novel finding from the patients study was demonstrated that LCK was largely increased in the liver cirrhosis tissues. Similar findings were shown in the fibrotic

liver tissues from CCl_4-treated mice. To identify the function of LCK on CCl_4-induced liver fibrosis mice, liver-specific LCK knockdown mice were used. The results showed that downregulation of LCK alleviated the degree of liver fibrosis compared to vehicle mice. Interestingly, LCK was significantly down-regulated in the regression of liver fibrosis in CCl_4-induced mice model. This was also supported by the findings that the expression of LCK was up-regulated in activated HSC (aHSC) and restored in inactivated HSC (iHSC), which was in accord with the expression of α-SMA or Col1α1. These data provided a new hypothesis that LCK may regulate the development of progression and reversal of liver fibrosis. Furthermore, knockdown LCK inhibited TGF-β1-induced proliferation of HSC, while overexpression of LCK inhibited activated HSC reverting to an inactivated phenotype induced by MDI. Thus, LCK mediated liver fibrosis may be a mechanism by activated HSC and reverting to an inactivated phenotype.

It was found SOCS1 had a high affinity in binding to the oncogenic LCK kinase (Venkitachalam et al. 2011). Cooper et al also reported enforced SOCS1 expression attenuated LCK-mediated cellular transformation (Cooper et al. 2010). SOCS1, a key regulator of immune cell activation, acts as a negative regulator of cytokine signals and plays a key role in the suppression of tissue injury and inflammatory diseases (Cheng et al. 2014). Kandhi et al found SOCS1 controled liver fibrosis by regulating HSC proliferation (Kandhi et al. 2016). The findings from Mafandais's group also supported the idea of the important function of SOCS1 in liver fibrosis (Kawila et al. 2018). Co-immunoprecipitation (Co-IP) result demonstrated LCK interacted with SOCS1. SOCS1 is an important negative regulatory protein in JAK1/STAT1/3 activator pathways, and also inhibits the signaling pathways of various cytokines. We observed that expression of p-JAK1 and p-STAT1/3 was enhanced in CCl_4-induced group, and decresed in AAV-LCK-treated group. In vitro model, when LCK was knocked down by siRNA, p-JAK1 and p-STAT1/3 were also reduced. Similarly, overexpression of LCK in HSCs, p-JAK1 and p-STAT1/3 were increased. Furthermore, in our previous study, overexpression of SOCS1 alleviated liver fibrosis (Zhu et al. 2021). Consistently, SOCS1 was indeed down-regulated in CCl_4-induced liver fibrosis and significantly up-regulated in spontaneously reversal mice group in our current study. Double immunofluorescence staining showed that knockdown of LCK promoted the expression of SOCS1 in rAAV9–LCK-treated liver fibrosis mice. Similar results were also supported by the data *in vitro*. Moreover, knockdown of LCK may up-regulate SOCS1 in TGF-β1-induced HSC-T6 cells, while overexpression of LCK in MDI-induced inactivated HSC-T6 cells down-regulated SOCS1 expression.

Taken together, our findings unveiled a novel function of LCK in liver fibrosis. LCK stimulated activation of HSC and obstructed the regression of activated HSC, which was at least partly mediated by SOCS1 (Fig. 9). Given the pivotal role of LCK in liver fibrosis progression and regression, it implied LCK as a potential therapeutic target for liver fibrosis treatment.

Abbreviations

AAV9 Adeno-associated viruses

ALT Alanine aminotransferase

AST	Aspartate aminotransferase
α-SMA	α-smooth muscle actin
CCl_4	carbon tetrachloride
COl1α1	Type I collagen
ECM	Extracellular matrix
HA	Hyaluronic Acid
HSC	Hepatic stellate cells
JAK1	Janus kinase-1
LCK	Lymphocyte-specific protein tyrosine kinase
LF	liver fibrosis
LN	laminin
PCIII	Type 3 procollagen
SiRNA	Small interfering RNA
SOCS1	Suppressor of cytokine signaling 1
STAT1	signal transducer and activator of transcription 1
STAT3	signal transducer and activator of transcription 3

Declarations

Acknowledgments The authors thank the Center for Scientific Research of Anhui Medical University for valuable help in our experiment.

Authors' Contributions C. Huang conceived the idea of the study, designed experiments, and wrote and edited the manuscript. T. Ma revised the manuscript. H. Zhao and H. Zhu designed and performed experiments, Y. Ding and Y. Zhang performed experiments.

Funding This work was supported by funding from the National Science Foundation of China (82070628) and the University Synergy Innovation Program of Anhui Province (GXXT-2019-045, GXXT-2020-063, GXXT-2020-025). The authors thank the Center for Scientific Research of Anhui Medical University for valuable help in our experiment.

Data Availability Statements

All data generated or analysed during this study are included in this published article (and its supplementary information files).

Availability of data and material (data transparency) Not applicable

Code availability (software application or custom code) Not applicable

Declarations

Ethics approval All protocols for animal experiments were approved by the Anhui Medical University Animal Care and Use Committee.

Consent to participate Not applicable.

Consent for publication Not applicable.

Conflict of interest The authors declare no competing interests.

References

1. Abraham N, M MC, P JR. and A. V Enhancement of T-cell responsiveness by the lymphocyte-specific tyrosine protein kinase p56lck. Nature. 1991. 350.
2. Berumen J, Baglieri J, Kisseleva T, Mekeel K. Liver fibrosis: Pathophysiology and clinical implications. WIREs Mech Dis. 2021;13:e1499. http://doi.org/10.1002/wsbm.1499.
3. Betapudi V, Shukla M, Alluri R, Merkulov S, Mccrae K R J F J O P O T F O a S. F E B. Novel role for p56/Lck in regulation of endothelial cell survival and angiogenesis. FASEB J. 2016;30:3515. http://doi.org/10.1096/fj.201500040.
4. Bommhardt U, Schraven B, Simeoni L, Beyond TCR, Signaling. Emerging Functions of Lck in Cancer and Immunotherapy. Int J Mol Sci. 2019. 20.http://doi.org/10.3390/ijms20143500.
5. Bu FT, Chen Y, Yu HX, Chen X, Yang Y, Pan XY, Wang Q, Wu YT, Huang C. Meng X M. SENP2 alleviates CCl4-induced liver fibrosis by promoting activated hepatic stellate cell apoptosis and reversion. Toxicol Lett. 2018;289:86–98. http://doi.org/10.1016/j.toxlet.2018.03.010.
6. Bu FT, Zhu Y, Chen X, Wang A, Li J, Circular RNA. circPSD3 alleviates hepatic fibrogenesis by regulating the miR-92b-3p/Smad7 axis. Mol Therapy - Nucleic Acids. 2021;23:847–62. http://doi.org/10.1016/j.omtn.2021.01.007.
7. Calvente CJ, Tameda M, Johnson CD, Pilar H, D,Feldstein A E J T J O C. I. Neutrophils contribute to spontaneous resolution of liver inflammation and fibrosis via microRNA-223. J Clin Investig. 2019. 130.http://doi.org/10.1172/JCI122258.

8. Cheng C, Huang C, Ma TT, Bian EB, He Y, Zhang L, Li J. SOCS1 hypermethylation mediated by DNMT1 is associated with lipopolysaccharide-induced inflammatory cytokines in macrophages. Toxicol Lett. 2014;225:488–97. http://doi.org/10.1016/j.toxlet.2013.12.023.
9. Cooper JC, Shi M, Chueh FY, Venkitachalam S, Yu CL. Enforced SOCS1 and SOCS3 expression attenuates Lck-mediated cellular transformation. Int J Oncol. 2010. 36.http://doi.org/10.3892/ijo_00000603.
10. Ginès P, Krag A, Abraldes JG, Solà E, Fabrellas N, Kamath PS. Liver cirrhosis. The Lancet. 2021;398:1359–76. http://doi.org/10.1016/s0140-6736(21)01374-x.
11. Kandhi R, Bobbala D, Yeganeh M, Mayhue M, Menendez A, Ilangumaran S. Negative regulation of the hepatic fibrogenic response by suppressor of cytokine signaling 1. Cytokine. 2016;82:58–69. http://doi.org/10.1016/j.cyto.2015.12.007.
12. Kawila ME, Rajani K, Diwakar B, Musawwir K, Madhuparna N, Alfredo M, Sheela R, Subburaj I. Essential role of suppressor of cytokine signaling 1 (SOCS1) in hepatocytes and macrophages in the regulation of liver fibrosis. Cytokine.2018:S1043466618303302-.http://doi.org/10.1016/j.cyto.2018.07.032.
13. Kisseleva T, Brenner D. Molecular and cellular mechanisms of liver fibrosis and its regression. Nat Rev Gastroenterol Hepatol. 2021;18:151–66. http://doi.org/10.1038/s41575-020-00372-7.
14. Kisseleva T, Brenner DA. Anti-fibrogenic strategies and the regression of fibrosis. Best Pract Res Clin Gastroenterol. 2011;25:305–17. http://doi.org/10.1016/j.bpg.2011.02.011.
15. Kisseleva T, Cong M, Paik Y, Scholten D, Jiang C, Benner C, Iwaisako K, Moore-Morris T, Scott B, Tsukamoto H, Evans SM, Dillmann W, Glass C. K,Brenner D A. Myofibroblasts revert to an inactive phenotype during regression of liver fibrosis. Proc Natl Acad Sci U S A. 2012;109:9448–53. http://doi.org/10.1073/pnas.1201840109.
16. Krizhanovsky V, Yon M, Dickins RA, Hearn S, Simon J, Miething C, Yee H, Zender L. Lowe S W. Senescence of Activated Stellate Cells Limits Liver Fibrosis. Cell. 2008;134:657–67. http://doi.org/10.1016/j.cell.2008.06.049.
17. Li L, Cui Y, Shen J, Dobson H, Sun G. Evidence for activated Lck protein tyrosine kinase as the driver of proliferation in acute myeloid leukemia cell, CTV-1. Leuk Res. 2019;78:12–20. http://doi.org/10.1016/j.leukres.2019.01.006.
18. Li X, Wu XQ, Xu T, Li XF, Yang Y, Li WX, Huang C, Meng XM, Li J. Role of histone deacetylases(HDACs) in progression and reversal of liver fibrosis. Toxicol Appl Pharmacol. 2016;306:58–68. http://doi.org/10.1016/j.taap.2016.07.003.
19. Liau N, Laktyushin A, Lucet IS, Murphy JM, Yao S, Whitlock E, Callaghan K, Nicola NA, Kershaw NJ, Babon JJ. The molecular basis of JAK/STAT inhibition by SOCS1. Nat Commun. 2018;9:1558. http://doi.org/10.1038/s41467-018-04013-1.
20. Liu J, Guo Z, Zhang Y, Wu T, Guo Z. LCK inhibitor attenuates atherosclerosis in ApoE mice via regulating T cell differentiation and reverse cholesterol transport. J Mol Cell Cardiol. 2020;139:87–97. http://doi.org/10.1016/j.yjmcc.2020.01.003.

21. Liu X, Wu Y, Yang Y, Li W, Huang C, Meng X, Li J. Role of NLRC5 in progression and reversal of hepatic fibrosis. Toxicol Appl Pharmacol. 2016;294:43–53. http://doi.org/10.1016/j.taap.2016.01.012.
22. Shi M, Cooper JC, Yu CL. A constitutively active Lck kinase promotes cell proliferation and resistance to apoptosis through signal transducer and activator of transcription 5b activation. Mol Cancer Res. 2006;4:39–45. http://doi.org/10.1158/1541-7786.MCR-05-0202.
23. Talab F, Allen JC, Thompson V, Lin K, Slupsky JR. LCK is an important mediator of B-cell receptor signaling in chronic lymphocytic leukemia cells. Mol Cancer Res. 2013;11:541–54. http://doi.org/10.1158/1541-7786.MCR-12-0415-T.
24. Tha B, Slf A, Yh A. Hepatic stellate cells as key target in liver fibrosis - ScienceDirect. Adv Drug Deliv Rev. 2017;121:27–42. http://doi.org/10.1016/j.addr.2017.05.007.
25. Tsuchida T, Friedman SL. Mechanisms of hepatic stellate cell activation. Nat Rev Gastroenterol Hepatol. 2017;14:397–411. http://doi.org/10.1038/nrgastro.2017.38.
26. Valeria R, Maluf, Daniel G, Cher A, Kellie J, Yanek. Kenneth, Kong, Xiangrong,Kulik. Genes Involved in Viral Carcinogenesis and Tumor Initiation in Hepatitis C Virus–Induced Hepatocellular Carcinoma. Mol Med. 2009;15:85–94. http://doi.org/10.2119/molmed.2008.00110.
27. Venkitachalam S, C FY, L KF. S. P, and C.L. Y Suppressor of cytokine signaling 1 interacts with oncogenic lymphocyte-specific protein tyrosine kinase. Oncol Rep. 2011. 25.http://doi.org/10.3892/or.2011.1144.
28. Wang S, Friedman SL. Hepatic fibrosis: A convergent response to liver injury that is reversible - ScienceDirect. J Hepatol. 2020;73:210–1. http://doi.org/10.1016/j.jhep.2020.03.011.
29. Wei Q, Brzostek J, Sankaran S, Casas J, Hew LS, Yap J, Zhao X, Wojciech L. and Gascoigne N R J Lck bound to coreceptor is less active than free Lck. Proc Natl Acad Sci U S A. 2020;117:15809–17. http://doi.org/10.1073/pnas.1913334117.
30. Wurmbach E, Chen YB, Khitrov G, Zhang W, Roayaie S, Schwartz M, Fiel I, Thung S, Mazzaferro V, Bruix J, Bottinger E, Friedman S, Waxman S, Llovet JM. Genome-wide molecular profiles of HCV-induced dysplasia and hepatocellular carcinoma. Hepatology. 2007;45:938–47. http://doi.org/10.1002/hep.21622.
31. Yang Y, Wu XQ, Li WX, Huang HM, Li HD, Pan XY, Li XF, Huang C, Meng XM, Zhang L. PSTPIP2 connects DNA methylation to macrophage polarization in CCL4-induced mouse model of hepatic fibrosis. Oncogene. 2018;37:6119–35. http://doi.org/10.1038/s41388-018-0383-0.
32. You H, Wang L, Bu F, Meng H, Pan X, Li J, Zhang Y, Wang A, Yin N, Huang C, Li JT. miR-455-3p/HDAC2 axis plays a pivotal role in the progression and reversal of liver fibrosis and is regulated by epigenetics. FASEB J. 2021;35:e21700. .http://doi.org/10.1096/fj.202002319RRR.
33. Yu HX, Yao Y, Bu FT, Chen Y, Wu YT, Yang Y, Chen X, Zhu Y, Wang Q, Pan XY, Meng XM, Huang C, Li J. Blockade of YAP alleviates hepatic fibrosis through accelerating apoptosis and reversion of activated hepatic stellate cells. Mol Immunol. 2019;107:29–40. http://doi.org/10.1016/j.molimm.2019.01.004.

34. Zepecki JP, Snyder KM, Moreno MM, Fajardo E, Fiser A, Ness J, Sarkar A, Toms SA, Tapinos N. Regulation of human glioma cell migration, tumor growth, and stemness gene expression using a Lck targeted inhibitor. Oncogene. 2018;38:1734–50. http://doi.org/10.1038/s41388-018-0546-z.
35. Zhu H, Zhao H, Xu S, Zhang Y, Ding Y, Li J, Huang C, Ma T. Sennoside A alleviates inflammatory responses by inhibiting the hypermethylation of SOCS1 in CCl4-induced liver fibrosis. Pharmacol Res. 2021;174:105926. http://doi.org/10.1016/j.phrs.2021.105926.

Figures

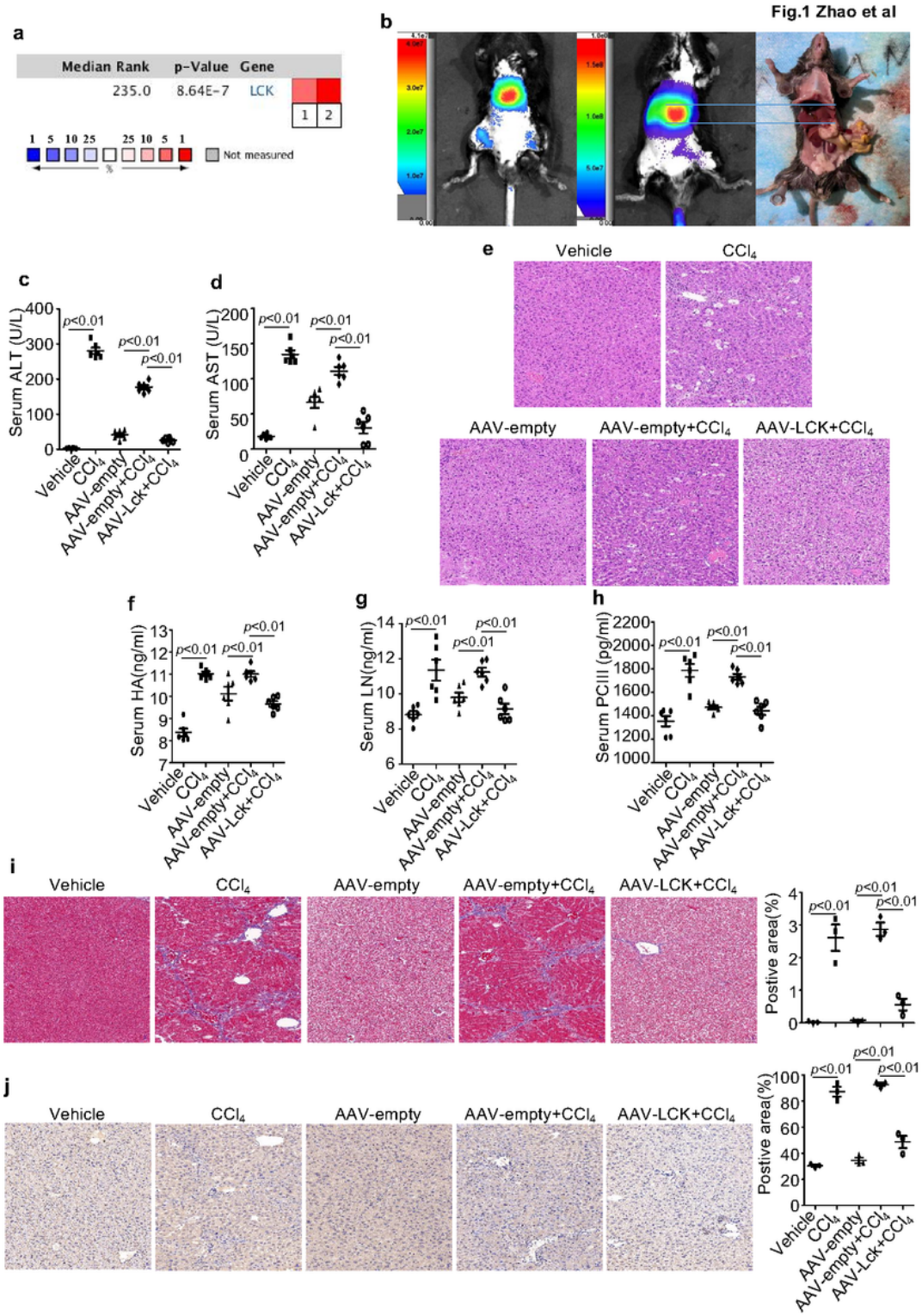

Figure 1

LCK promotes CCl4-induced liver fibrosis.

a A meta-analysis of LCK gene expression from two Oncomine databases where colored squares indicate the median rank for LCK (vs. Normal tissue) across 2 analyses. The p value is given for the median rank analysis.

b Fluorescence-labelled rAAV9–LCK was localized in liver.

c Serum levels of ALT in different groups.

d Serum levels of AST in different groups.

e H&E staining of liver tissues in different groups. Magnification: 20×.

f Serum levels of HA in different groups.

g Serum levels of LN in different groups.

h Serum levels of PCIII in different groups.

i Masson staining of liver tissues in different groups. The positive staining areas were measured by Image-Pro Plus 6.0 (Media Cybernetics, Inc, Rockville, MD, USA). Magnification: 20×.

j Immunohistochemistry of Col1α1 in different groups of liver tissues. The positive staining areas were measured by Image-Pro Plus 6.0 (Media Cybernetics, Inc, Rockville, MD, USA). Magnification: 20×.

Similar results were obtained in 3 independent experiments with 10 mice per group.

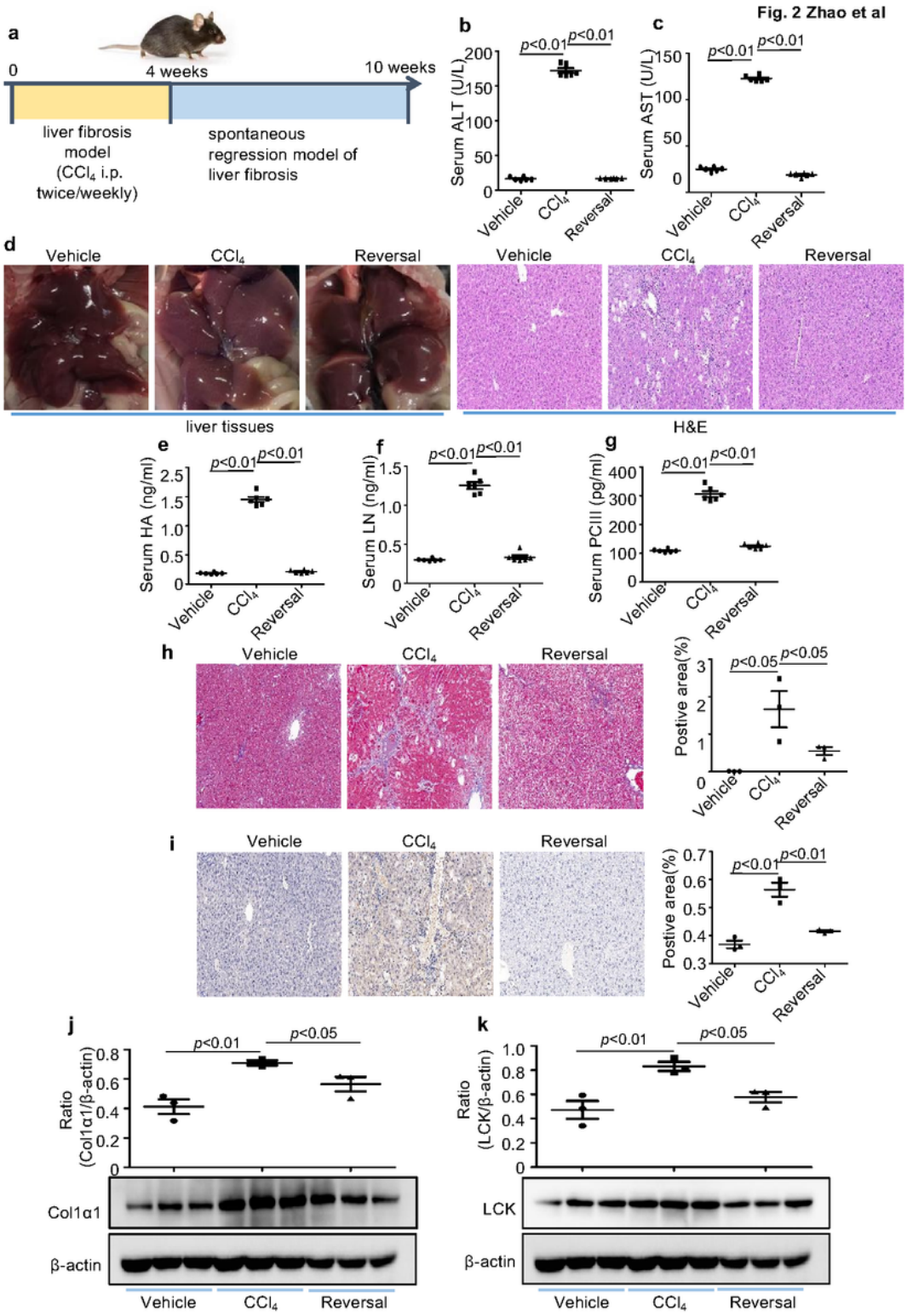

Figure 2

Regression of liver fibrosis is accompanied by loss of LCK in vivo.

a Establishment of spontaneous liver fibrosis regression mice model.

b Serum levels of ALT in different groups.

c Serum levels of AST in different groups.

d Representative macroscopic appearance of the liver and H&E staining of liver tissues. Magnification: 20×.

e Serum levels of HA in different groups.

f Serum levels of LN in different groups.

g Serum levels of PCIII in different groups.

h Masson staining of liver tissues in different groups. The positive staining areas were measured by Image-Pro Plus 6.0 (Media Cybernetics, Inc, Rockville, MD, USA). Magnification: 20×.

i Immunohistochemistry of Col1α1 in different groups of liver tissues. The positive staining areas were measured by Image-Pro Plus 6.0 (Media Cybernetics, Inc, Rockville, MD, USA). Magnification: 20×.

j The expression level of Col1α1 in different groups.

k The expression level of LCK in different groups.

Similar results were obtained in 3 independent experiments with 10 mice per group.

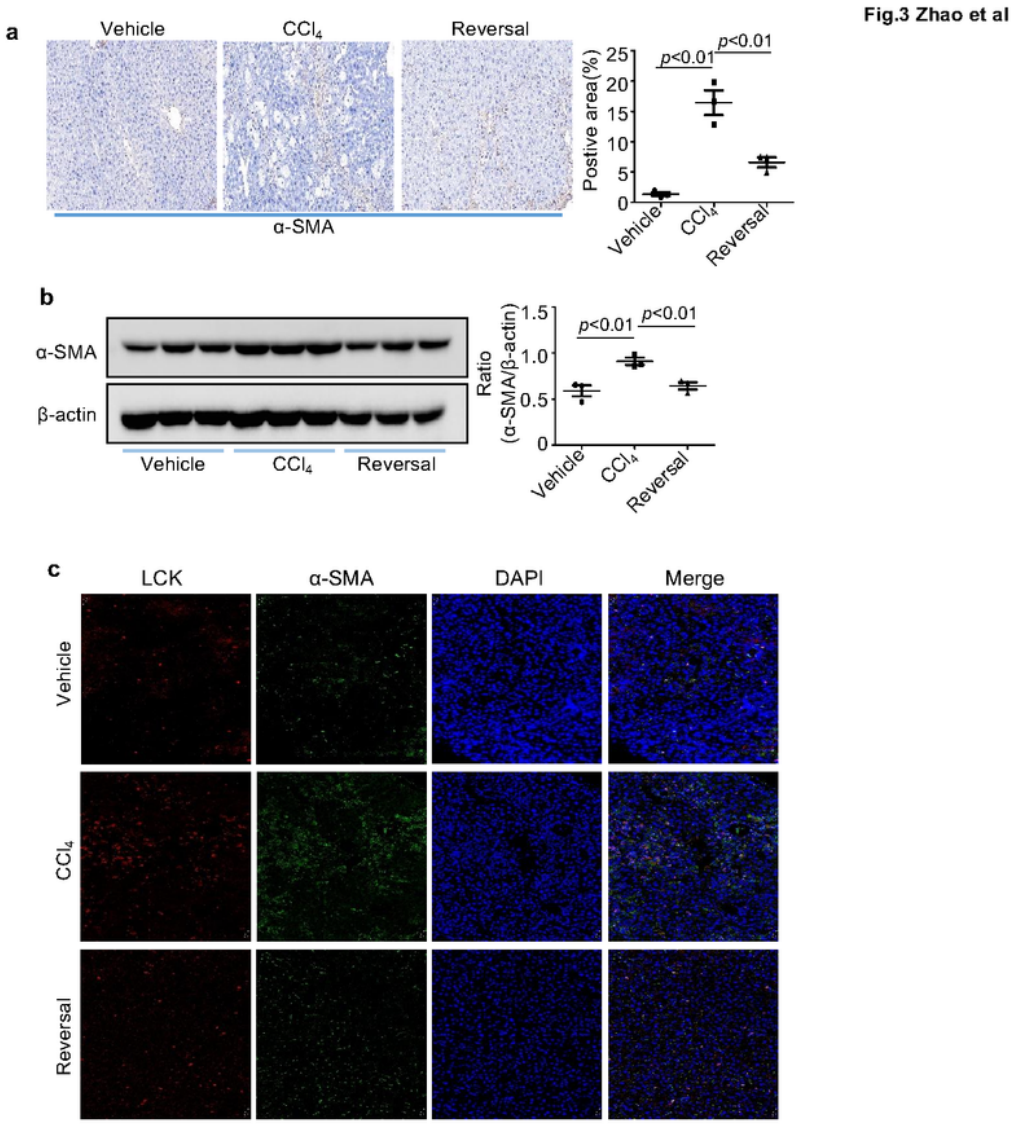

Figure 3

LCK was colocalized with α-SMA in the process of liver fibrosis.

a Immunohistochemistry of α-SMA in different groups of liver tissues. The positive staining areas were measured by Image-Pro Plus 6.0 (Media Cybernetics, Inc, Rockville, MD, USA). Magnification: 20 ×.

b The protein levels of α-SMA in different groups.

c Colocalization of LCK and α-SMA in the liver tissues. Magnification: 20×.

Similar results were obtained in 3 independent experiments with 10 mice per group.

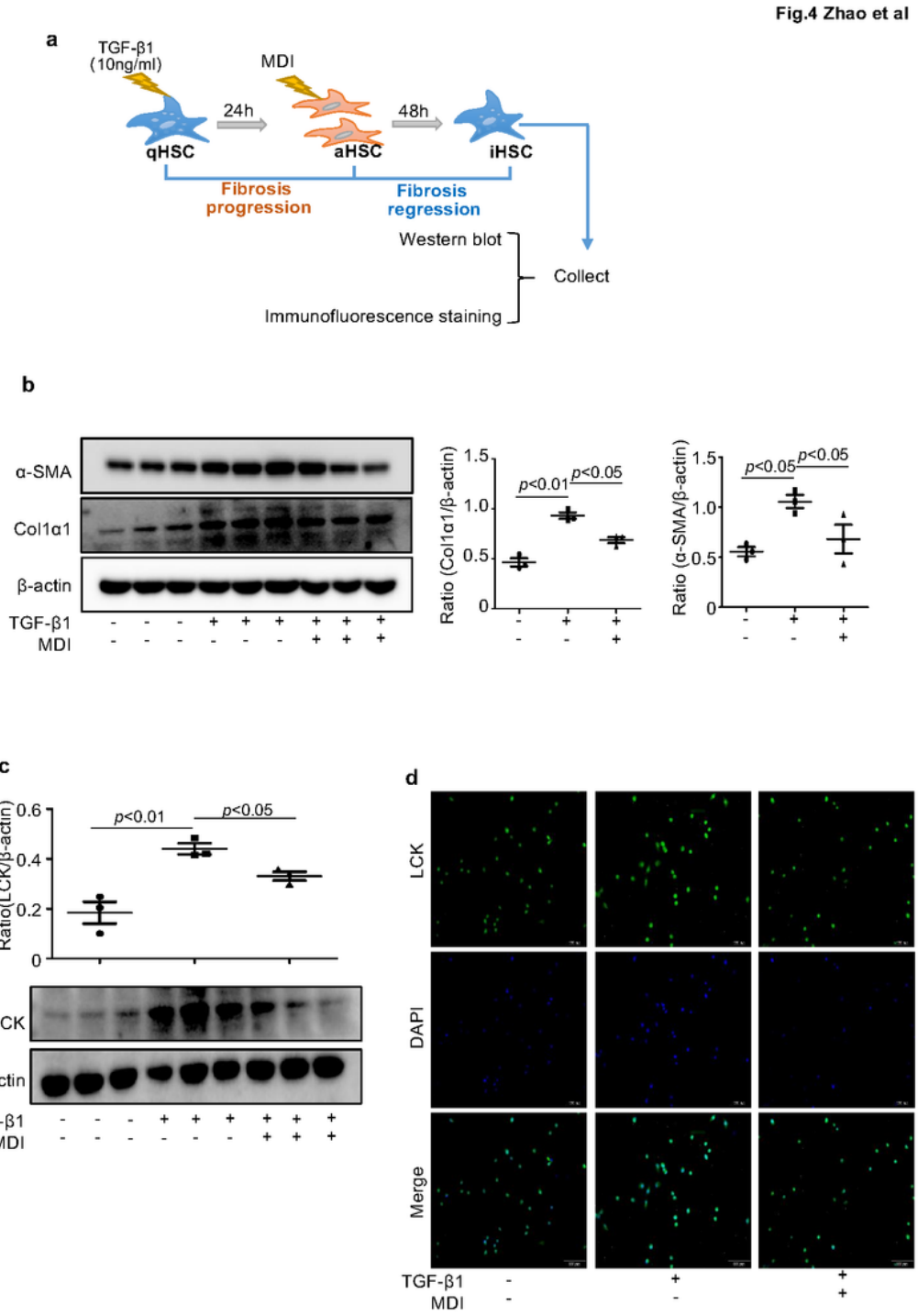

Figure 4

Regression of liver fibrosis is accompanied by loss of LCK in vitro.

a HSC-T6 cells were induced by TGF-β1 (10 ng/ml) in advance and 24 hours later, exposed to MDI for 48 hours.

b The protein levels of α-SMA and Col1α1were detected by western blot.

c The protein levels of LCK was detected by western blot.

d Expression of LCK in HSC-T6 cells by immunofluorescence staining. Magnification: 100×.

Similar results were obtained in triplicate culture assays.

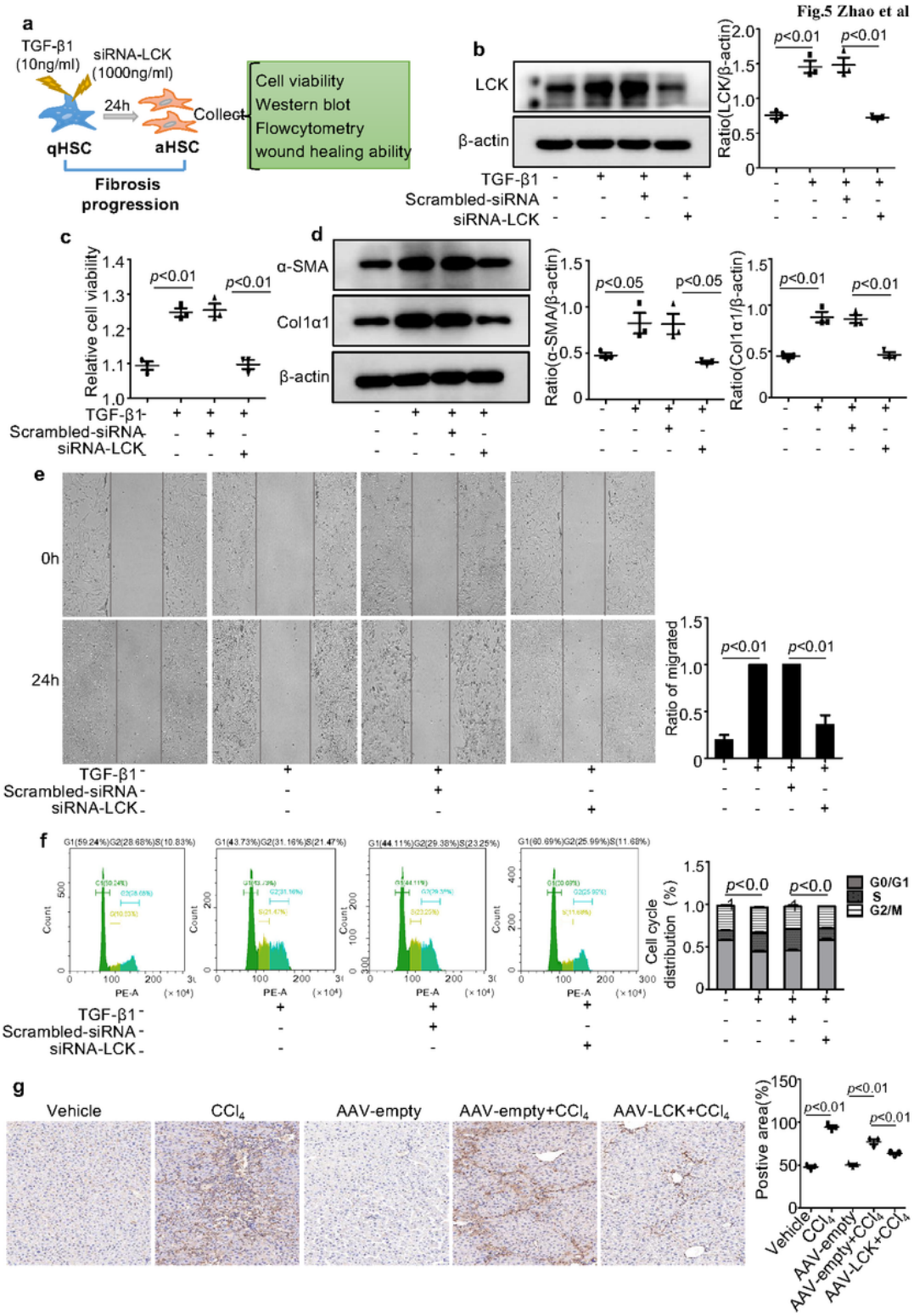

Figure 5

Knockdown of LCK inhibited the proliferation of HSC.

a HSC-T6 cells were induced by TGF-β1 (10 ng/ml) and siRNA-LCK for 24 hours.

b Protein level of LCK in HSC-T6 cells treated with siRNA-LCK by western blot.

c The relative cell viability of HSC-T6 cells treated with siRNA-LCK by CCK8.

d Protein levels of Col1α1 and α-SMA in HSC-T6 cells treated with siRNA-LCK by western blot.

e The migration was determined in HSC-T6 cells treated with siRNA-LCK.

f The cell cycle was detected in HSC-T6 cells treated with siRNA-LCK by flow cytometry.

g Immunohistochemistry of α-SMA in different groups of liver tissues. The positive staining areas were measured by Image-Pro Plus 6.0 (Media Cybernetics, Inc, Rockville, MD, USA). Magnification: 20×.

Similar results were obtained in 3 independent experiments with 10 mice per group or obtained in triplicate culture assays.

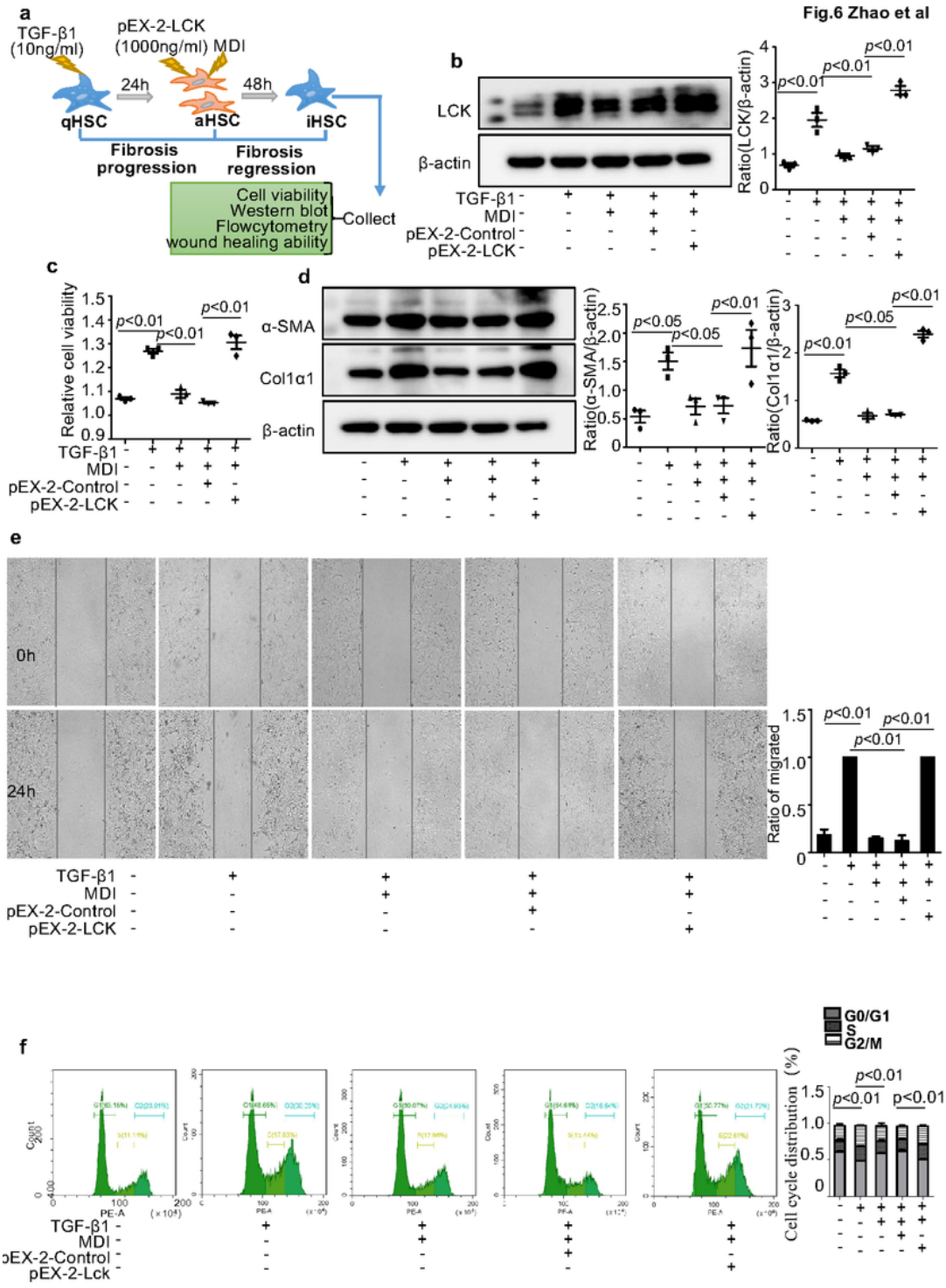

Figure 6

Overexpression of LCK inhibited activated HSC going to inactivated phenotype.

a HSC-T6 cells were treated with TGF-β1 (10 ng/ml) for 24 hours, then induced by pEX-2-LCK and MDI for 48 hours.

b Protein level of LCK in HSC-T6 cells treated with pEX-2-LCK by western blot.

c The relative cell viability of HSC-T6 cells treated with pEX-2-LCK by CCK8.

d Protein levels of Col1α1 and α-SMA in HSC-T6 cells treated with pEX-2-LCK by western blot.

e The migration was determined in HSC-T6 cells treated with pEX-2-LCK.

f The cell cycle was detected in HSC-T6 cells treated with pEX-2-LCK by flow cytometry.

Similar results were obtained in triplicate culture assays.

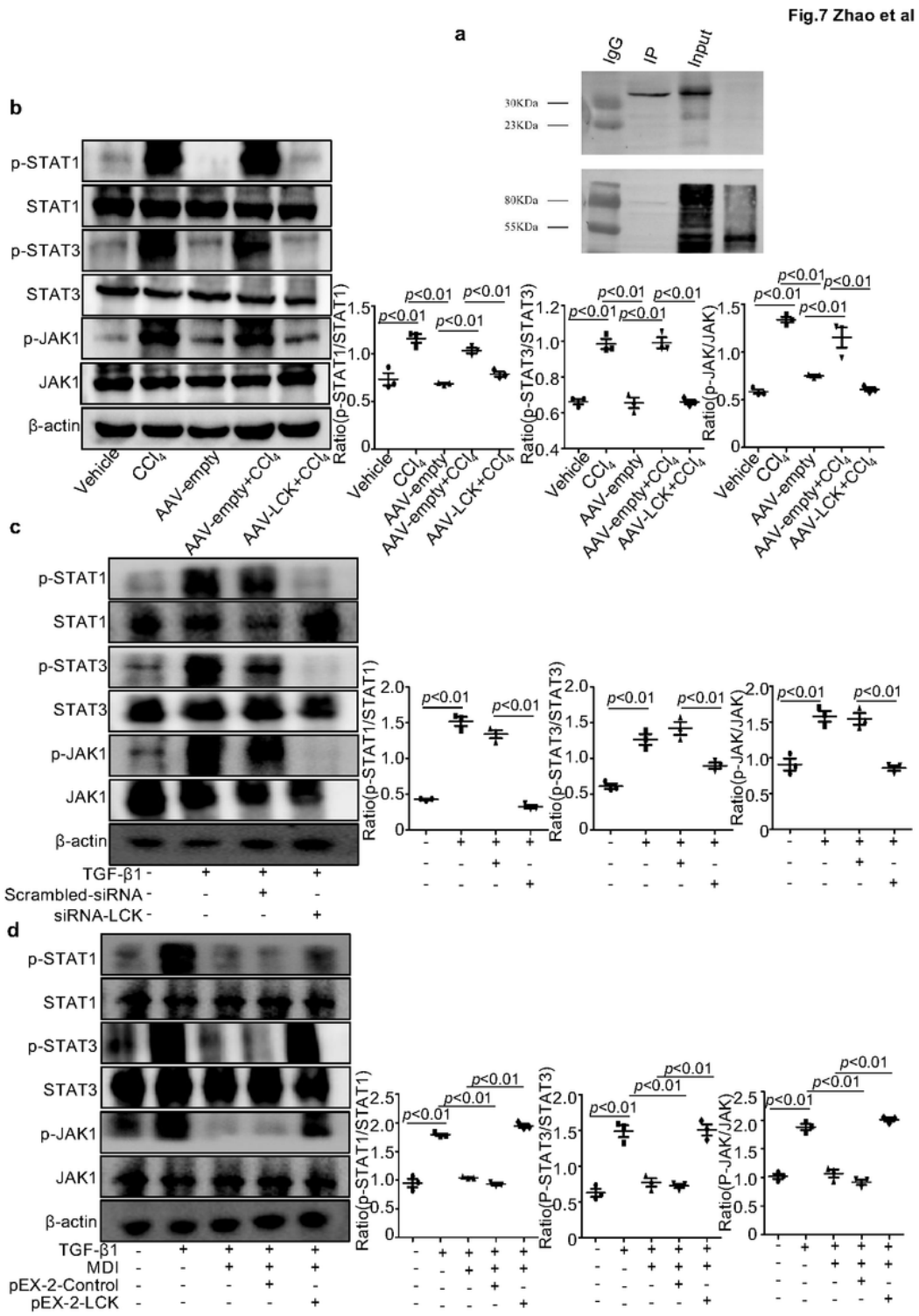

Figure 7

LCK interacted with SOCS1.

a LCK interacted with SOCS1 by Co-IP.

b The expression of p-STAT1, STAT1, STAT3, p-STAT3, JAK1, p-JAK1 from liver tissue in different groups.

c Protein levels of p-STAT1, STAT1, STAT3, p-STAT3, JAK1, p-JAK1 in HSC-T6 cells treated with siRNA-LCK by western blot.

d Protein levels of p-STAT1, STAT1, STAT3, p-STAT3, JAK1, p-JAK1 in HSC-T6 cells treated with pEX-2-LCK by western blot.

Similar results were obtained in 3 independent experiments with 10 mice per group or in triplicate culture assays.

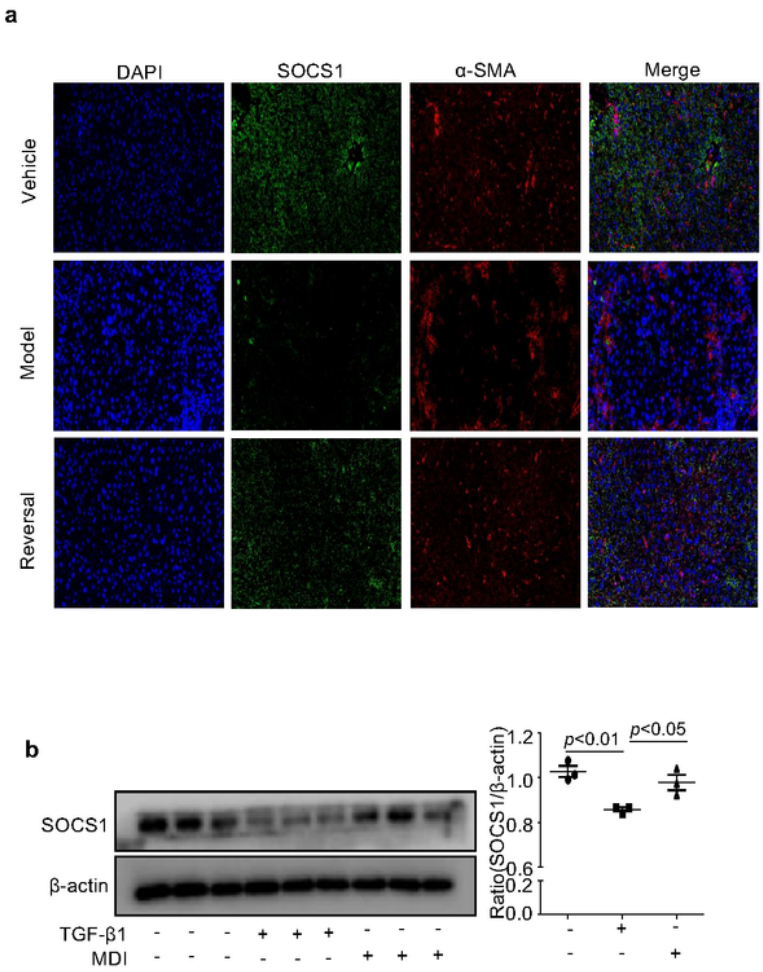

Figure 8

SOCS1 protein level was increased in model group and deceased in reversal group.

a Colocalization of SOCS1 and α-SMA in the liver tissues. Magnification: 20×

b The protein level of SOCS1 in HSC-T6 cells.

Similar results were obtained in 3 independent experiments with 10 mice per group or in triplicate culture assays.

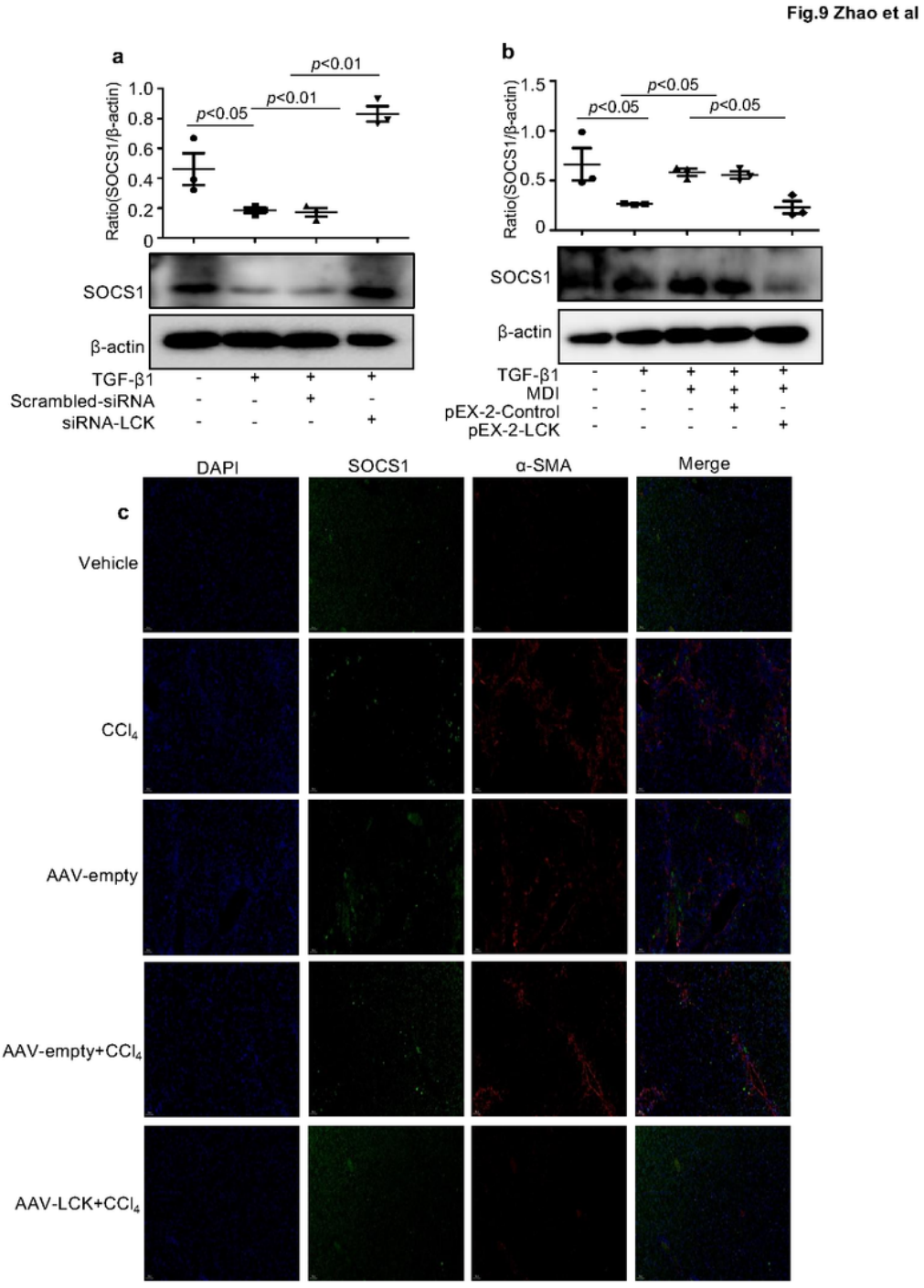

Figure 9

LCK stimulated activation of HSC and obstructed the regression of activated HSC, which was at least partly mediated by SOCS1.

a Protein level of SOCS1 in HSC-T6 cells treated with siRNA-LCK.

b Protein level of SOCS1 in HSC-T6 cells treated with pEX-2-LCK.

c Colocalization of SOCS1 and α-SMA in the liver tissues. Magnification: 20×.

Similar results were obtained in 3 independent experiments with 10 mice per group or in triplicate culture assays.

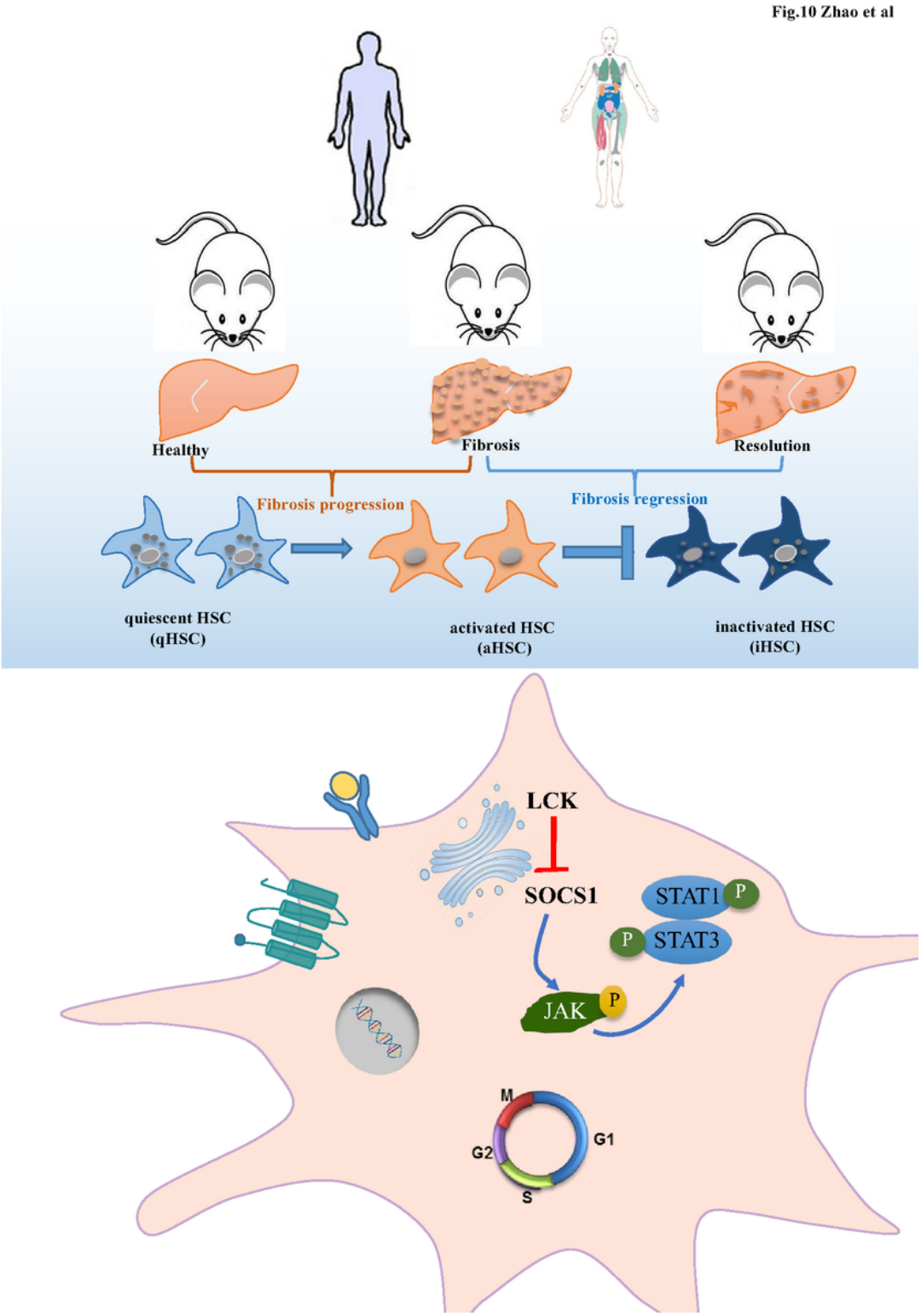

Figure 10

Legend not included with this version.